Angle-dependent reversible and irreversible magnetic torque in single-crystalline $Y_2Ba_4Cu_8O_{16}$

D. Zech*
Physik-Institut, University of Zürich, Winterthurerstrasse 190, 8057 Zürich, Switzerland

C. Rossel and L. Lesne
IBM Research Division, Zurich Research Laboratory, 8803 Rüschlikon, Switzerland

H. Keller and S. L. Lee
Physik-Institut, University of Zürich, Winterthurerstrasse 190, 8057 Zürich, Switzerland

J. Karpinski
Laboratorium für Festkörperphysik, Eidgenössische Technische Hochschule Zürich, 8093 Zürich, Switzerland
(Received 22 June 1995; revised manuscript received 26 June 1996)

A systematic study of the angle-dependent reversible and irreversible magnetic torque in single-crystalline $Y_2Ba_4Cu_8O_{16}$ is presented. The high purity of the crystals allows us to show some intrinsic pinning properties of vortices due to the layered crystal structure. The irreversible component of the torque, which is unusually small, exhibits a peculiar angular dependence: It is minimal as the magnetic field B is applied along the ab plane and displays a pronounced maximum at finite angles, reminiscent of the ''fishtail'' effect. The unusual shape of the irreversible torque is attributed to the pinning of the vortex core, which becomes discontinuous below the two- to three-dimensional (2D-3D) crossover temperature. Another property shown by the angle-dependent torque is the lock-in of the vortex lines between the CuO_2 layers for B parallel to the ab plane. Applying the anisotropic 3D London model to fit the reversible torque data, we derive the in-plane London penetration depth $\lambda_{ab}=143$ nm, the coherence length $\xi_{ab}=1.9$ nm, and the effective mass anisotropy ratio $\gamma=12.3$ for $Y_2Ba_4Cu_8O_{16}$. [S0163-1829(96)02442-3]

I. INTRODUCTION

The cuprate superconductors are layered compounds built from stacks of superconducting CuO_2 planes separated by insulating or conducting buffer layers which serve as a charge reservoir. Due to their structure, the normal and superconducting properties of the cuprates exhibit a large anisotropy when measured parallel (ab) and perpendicular (c) to the CuO_2 planes. In the anisotropic Ginzburg-Landau or London model this anisotropy is described by an effective mass ratio $\gamma=\sqrt{m_c^*/m_{ab}^*}$, which is also the ratio λ_c/λ_{ab} and ξ_{ab}/ξ_c of the penetration depth and of the coherence length, respectively. In this approach vortex lines and their core are considered as continuous straight objects. The discreteness of the vortex structure becomes relevant only in the case of very large anisotropy. In this situation the core of a vortex line is discontinuous and consists of a stack of weakly coupled pancake vortices residing in the CuO_2 planes and the two-dimensional (2D) Lawrence-Doniach-type model is more appropriate. A comprehensive review on this subject is given by Blatter *et al.*[1] A useful criterion to distinguish between the above two cases is to compare the coherence length ξ_c along the c axis with the interlayer distance d. For $\xi_c<d$ the carrier density is modulated perpendicular to the planes, with a high density in the CuO_2 layers and a lower density between them. In fact, for the cuprates this is the case over a wide range of temperature. The modulation of the vortex cores leads to new phenomena in the vortex phase, and one expects that the anisotropic three-dimensional (3D) model does not strictly apply.[1,2] The experimental verification, however, remains difficult due to the presence of a large pinning background due to lattice defects or vacancies which completely blur the expected tiny deviations from the anisotropic 3D model.[3–8] As shown here, the $Y_2Ba_4Cu_8O_{16}$ (248) compound is an attractive system to explore the vortex-phase diagram of a layered cuprate superconductor with moderate anisotropy. As compared to the related $YBa_2Cu_3O_x$ system, the 248 compound has the advantages of a stoichiometric oxygen content and a stable structure with double CuO chains along the b axis, which prevents the formation of the detrimental twin-plane defects. These twin boundaries as well as lattice defects or oxygen vacancies have a strong influence on the vortex behavior due to their role as pinning centers.

In this work we present angle-dependent magnetic torque measurements on single-crystalline 248. We compare the reversible and irreversible torque for ''clean'' and Al-doped crystals and show that in the latter case already 1% Al impurities in the CuO_2 layers give rise to large pinning. In the ''clean'' crystals, however, pinning is extremely low, which allows us to study the interplay between the vortex lines and cores and the layered structure of the material. The angular dependence of the reversible and irreversible torque exhibits unexpected features which we discuss within the framework of the anisotropic 3D and the 2D models. From the reversible torque data we further derive the basic superconducting parameters such as the London penetration depth λ_{ab}, the effective mass anisotropy ratio γ, and an estimate of the in-plane coherence length ξ_{ab}.

II. EXPERIMENTAL DETAILS

Single-crystalline $Y_2Ba_4Cu_8O_{16}$ samples having approximate dimensions of $1\times1\times0.1$ mm^3 were grown in an

Y_2O_3 crucible by means of a high-pressure technique.[9] The critical temperature T_c determined by low-field superconducting quantum interference device (SQUID) magnetization measurements was 78.8 K with a width ΔT_c (10%–90%) of 3 K. A second set of samples was grown in an Al_2O_3 crucible. The somewhat lower critical temperature ($T_c = 73.8$ K) of these samples is caused by a small amount ($<1\%$) of Al impurities that diffuse from the crucible into the crystals and occupy preferentially the Cu(2) sites on the CuO_2 planes.[10]

Angle-dependent magnetization measurements have been performed on a noncommercial torque magnetometer with a capacitive torque detection having a sensitivity better than 10^{-9} Nm.[11] The setup allows continuous angle-dependent torque measurements in fields of $B<1.5$ T with an angular resolution of 0.01°. Initially, the sample was cooled in a field B applied parallel to the c axis ($\theta = 90°$). Temperature stability was better than 0.1 K. Then, angle-dependent measurements have been carried out by rotating the field B (0.5°/s) with respect to the sample ab plane while continuously monitoring the torque signal. Data were taken for both directions of rotation. From the experimental data the reversible and irreversible torque components (τ_{rev}, τ_{irr}) are derived in the usual way,

$$\tau_{rev}(\theta) = \tfrac{1}{2}[\tau^+(\theta) + \tau^-(\theta)], \tag{1a}$$

$$\tau_{irr}(\theta) = \tfrac{1}{2}[\tau^+(\theta) - \tau^-(\theta)], \tag{1b}$$

where $\tau^+(\theta)$ and $\tau^-(\theta)$ are the torque signals for the clockwise and counterclockwise directions of rotation, and θ is the angle between the applied field and the ab plane.[7,12] The irreversible component of the torque τ_{irr} is the width of the hysteresis and is a measure of an effective pinning force. The reversible torque τ_{rev} is the mean of the torque signal and is proportional to the equilibrium magnetization which is related to the fundamental superconducting parameters.

III. UNCONVENTIONAL TORQUE IN CLEAN $Y_2Ba_4Cu_8O_{16}$

Angle-dependent torque measurements on a clean 248 crystal (grown in Y_2O_3 crucible) have been carried out in the temperature range 48 K$<T<T_c$ and for applied fields between $B = 0.5$ and 1.4 T. Some of the measurements taken at either fixed field or constant temperature are shown in Figs. 1 and 2. Identical results were obtained on other 248 crystals with various shapes and picked from different batches. This demonstrates that the present torque data are indeed intrinsic to the clean 248 phase. The torque curves shown in Figs. 1 and 2 are unconventional in several respects. The most surprising feature is the very low irreversibility (width of hysteresis). As seen in Fig. 1, the irreversibility remains small even at $T \ll T_c$ and increases only slightly with decreasing temperature. The maximum seen in $\tau(\theta)$ broadens and shifts towards $\theta = \pm 90°$ as the temperature is decreasing. However, τ_{irr} obtained from the decomposition given in Eq. (1) remains for all angles and all temperatures much smaller than the corresponding reversible torque τ_{rev}. This is even true for $T<40$ K where a sharp and pronounced peak becomes apparent for the field applied close to the ab plane [see Fig. 1(c)]. An unusual angular dependence of the torque is also observed in the data taken at a fixed temperature. As

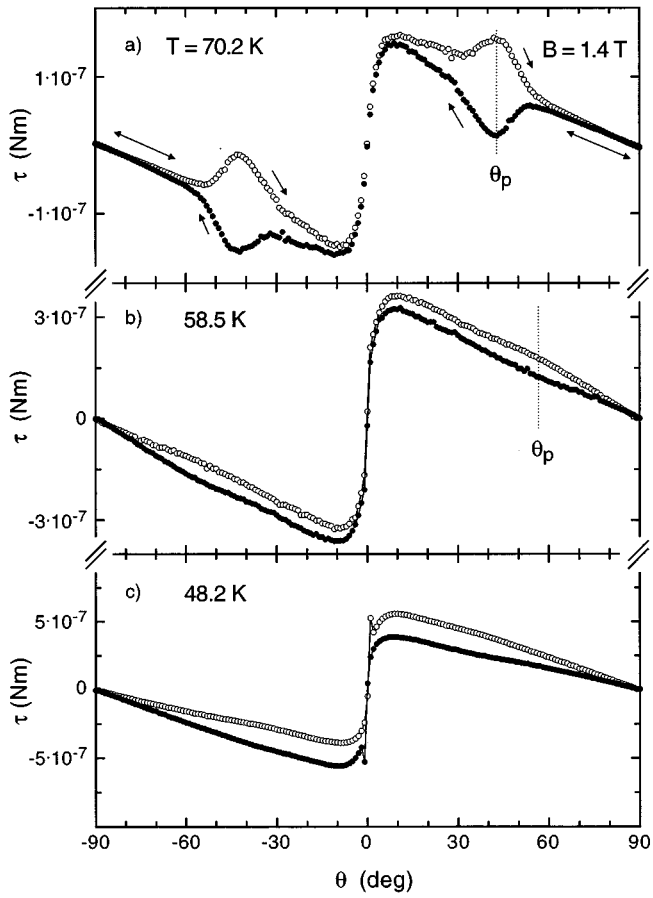

FIG. 1. Angle-dependent torque τ of a ''clean'' 248 single crystal for $T = 70.2$, 58.5, and 48.2 K and for fixed applied field $B = 1.4$ T. The arrows indicate the direction of rotation. θ_p denotes the angle for which the irreversible torque shows a maximum. For $\theta = 0°$ the field is parallel to the ab plane. Note that in (c) the sharp peak for $\theta \approx 0.5°$ is displayed on an enlarged scale in Fig. 7.

seen in Fig. 2 the irreversibility in the torque curves tends to decrease as the field is reduced from 1.4 to 0.5 T. This contrasts with the usual strong enhancement of irreversibility expected with decreasing field or temperature. Again, the maximum in τ_{irr} shifts towards $\theta = \pm 90°$ as the field is reduced, and finally disappears for $B<0.5$ T.

The low irreversible component in the torque and its unusual angular dependence are a rather unique property of 248. However, we believe that similar features in the torque would also be observed in other cuprates of low enough intrinsic disorder. In order to illustrate this further, we compare in Fig. 3(a) the data for the clean 248 crystal with those obtained for an Al-doped 248 single crystal, taken at the same reduced temperature $T/T_c = 0.92$ and in the field $B = 1.4$ T. In this sample less than 1% of copper sites are replaced by Al. In contrast to the clean sample the Al-doped sample exhibits a very large hysteresis which increases as the field is rotated towards the ab plane. This rather conventional behavior is analogous to that typically observed in cuprate superconductors (e.g., $YBa_2Cu_3O_x$) where intrinsic lattice imperfections such as oxygen vacancies or twin-plane boundaries give rise to considerably large pinning. In 248 a small density of point defects is already enough to produce a large irreversibility in the torque. This now suggest, that a

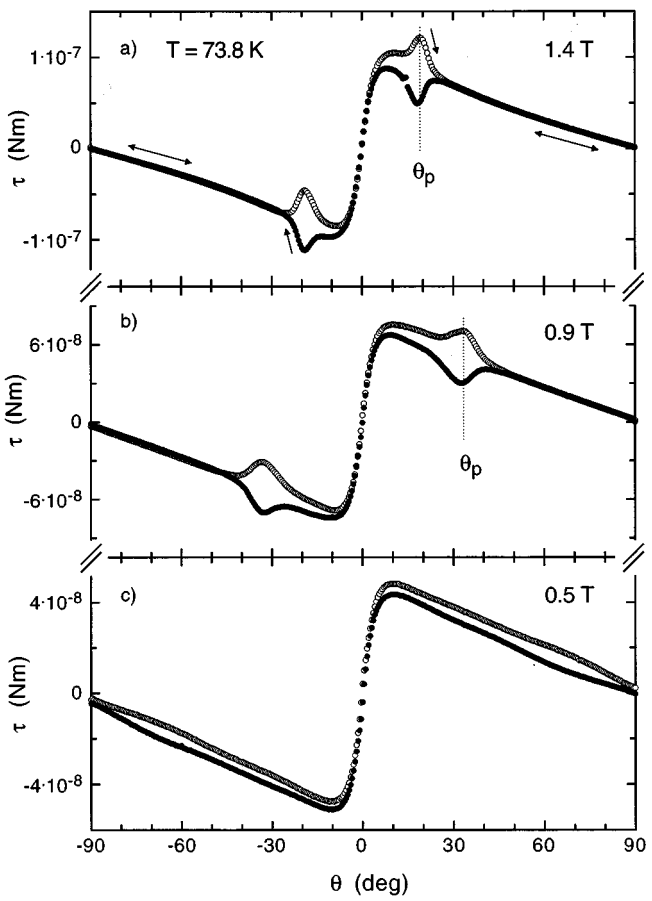

FIG. 2. Angle-dependent torque τ of a ''clean'' 248 single crystal at fixed temperature $T=73.8$ K and for an applied field of $B=1.4$, 0.9, and 0.5 T. The arrows indicate the direction of rotation. For $\theta=0°$ the field is parallel to the ab plane. θ_p denotes the angle for which the irreversible torque shows a maximum.

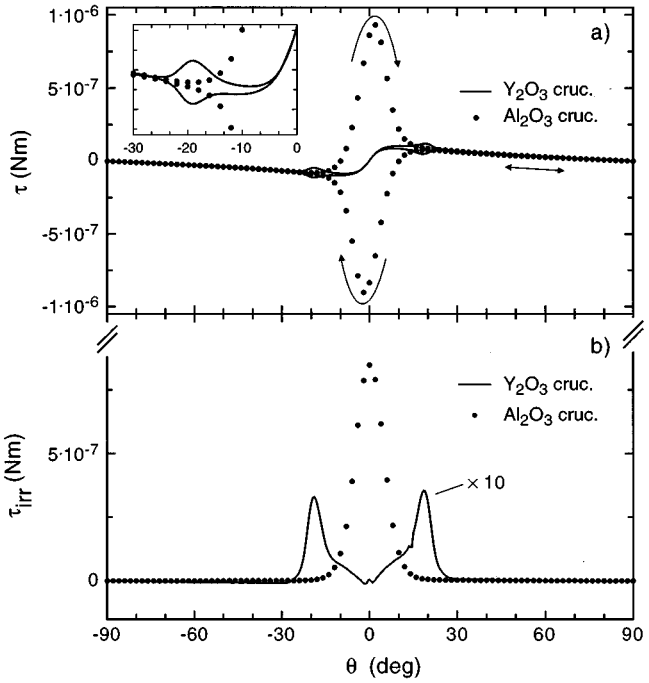

FIG. 3. (a) Angle-dependent torque at $T/T_c=0.92$ and $B=1.4$ T for ''clean'' 248 single crystal compared to an Al-doped 248 crystal. In the latter, isotropic pinning leads to a large irreversible torque at field orientations close to the ab plane. The enlarged scale near the angle where the torque becomes reversible is shown in the inset. (b) Irreversible component of the above torque data as derived from Eq. (2b). Note the enlarged scale for the clean 248 sample.

high reversibility in the torque can only be achieved in samples with very low intrinsic disorder as is the case for our stoichiometric 248 compound. Interestingly, although pinning in the Al-doped sample is significantly enhanced, the onset of the hysteresis at $\theta\simeq 25°$ is not affected by the increased disorder [see inset of Fig. 3(a)], and for $|\theta|>25°$ the reversible torque for both samples is identical. This interesting result, which may give some clues on the nature of the transition from the reversible to the irreversible part of the the vortex phase diagram, will be discussed elsewhere. In Fig. 3(b) we compare $\tau_{\rm irr}$ of the clean and Al-doped 248 samples. In the Al-doped sample the magnitude and shape of $\tau_{\rm irr}(\theta)$ are very different as compared to the clean sample. The Al-doped sample displays only one broad maximum at $\theta\simeq 0°$ as compared to the two maxima at $\theta_p\simeq\pm 20°$ observed in the clean sample. In fact, in the clean sample $\tau_{\rm irr}$ even vanishes for $\theta\simeq 0°$, whereas in the Al-doped sample $\tau_{\rm irr}$ becomes maximal. The very different behavior of the two samples clearly demonstrates the important role of point disorder in magnetic hystereses measurements. It further indicates that the unconventional angle-dependent torque in the clean sample cannot be understood within the framework of pinning due to point defects valid for the Al-doped sample.

Anomalous magnetic hysteresis in 248 single crystals were reported before by Xu *et al.*[13] They showed that down to 30 K the hysteresis in $M(B)$ remains small for fields $B<1$ T applied along the c axis, whereas a sharp increase of irreversibility appears at $B>1$ T. This ''fishtail'' behavior was interpreted in terms of weak surface barrier effects dominating at low fields and conventional bulk pinning setting in at higher fields. This behavior observed in the magnetic hysteresis is similar to the anomalous torque curves observed in the present experiment. In fact, the angle-dependent torque measurements are complementary to magnetization-loop measurements. In the first case, the magnetic flux is rotated at a fixed density of vortex lines while in magnetic hysteresis measurements the density of vortex lines is changed for a fixed sample orientation. Our torque data now indicate that the anomalous ''fishtail'' is not only determined by the strength of the applied field but also by its orientation with respect to the CuO_2 planes.

We now discuss the unconventional angular dependence of the torque signal in the clean 248 sample, as displayed in Figs. 1 and 2. First we compare the irreversible torque data with the anisotropic 3D model. As shown by Blatter *et al.*[14] the physical properties for an arbitrary orientation of the applied field are obtained from the known properties in the c-axis direction and by applying a simple angular scaling rule. The 3D anisotropic model is valid as much as London screening currents are concerned (see Sec. IV). However, it is not appropriate for describing the angular dependence of $\tau_{\rm irr}$ in the clean 248 sample which differs from the usual bulk pinning effects seen in the ''dirtier'' sample. Indeed, $\tau_{\rm irr}(\theta)$

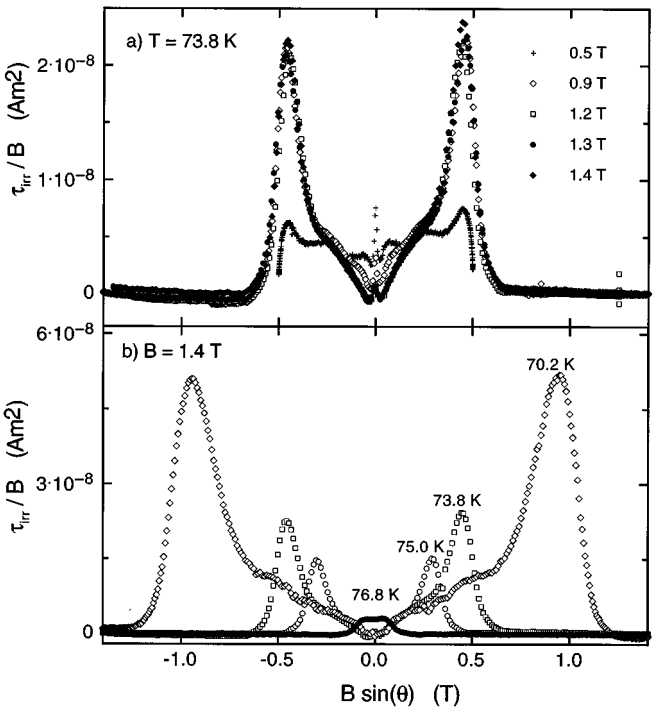

FIG. 4. (a) Scaling of the irreversible torque $\tau_{\rm irr}/B$ plotted as a function of the c-axis component of the field $B^c=B\sin\theta$ for an applied field of $B=1.4$, 1.3, 1.2, 0.9, and 0.5 T. (b) $\tau_{\rm irr}/B$ vs B^c measured at $B=1.4$ T and for the temperatures 70.2, 73.8, 75.0, and 76.8 K. Note that at $T=76.8$ K the shape of the irreversible torque is very different from the data taken at lower T.

in the clean sample decreases at lower θ, or equivalently its critical current density $j_c(\theta)$ decreases instead of reaching a broad maximum at $\theta=0°$ like in the Al-doped sample. This breakdown of the 3D scaling strongly suggests that the assumption of continuous vortex lines and cores made in the 3D anisotropic model is no more valid. This is the case in layered high-T_c superconductors below the 2D-3D crossover temperature $T_{\rm 2D\text{-}3D}$ when the coherence length $\xi_c(T)$ becomes shorter than the CuO_2 interlayer spacing d. For the 248 compound, the crossover temperature can be calculated to be $T_{\rm 2D\text{-}3D}\simeq T_c[1-2\xi_{ab}^2/(\gamma d)^2]=76.8$ K, using the parameters $\gamma=12.3$, $\xi_{ab}=1.9$ nm, $d=1.35$ nm, and $T_c=78.8$ K. Below $T_{\rm 2D\text{-}3D}$ the vortex lines are still straight and continuous objects, but the vortex cores, which are the relevant part for pinning become discontinuous. Pinning then involves 2D vortex cores in the CuO_2 layers and one would expect the properties related to pinning to scale with the c-axis component of the applied field (2D scaling).

In Fig. 4(a) the irreversible torque of the clean 248 sample, $\tau_{\rm irr}/B$, is plotted as a function of the field projection in the c-axis direction $B^c=B\sin\theta$ and for the temperature $T=73.8$ K. For the fields $B=1.4$, 1.3, 1.2, and 0.9 T the broad peaks almost completely overlap and the maximum irreversible torque occurs for the same field component B^c. Note also that the width of the maximum is the same after rescaling the data. For $B^c\to 0$ the irreversible torque is decreasing. This corresponds exactly to the low irreversibility found in the magnetic hysteresis at low fields.[13] However, in our case the magnitude of the applied field has not changed. Deviations from the 2D scaling are only observed for $B^c\approx 0°$ when B is almost parallel to the ab plane and where the interplay between vortex lines and the layered material structure becomes important (see Sec. V). For the measurement taken at $B=0.5$ T the irreversible torque is not fully developed, because the applied field of $B=0.5$ T is just at the onset of the ''fishtail'' behavior observed in the magnetization hysteresis loop. Nevertheless, the small maximum in $\tau_{\rm irr}$ is at the same position as for the experiments at higher fields. The 2D scaling of $\tau_{\rm irr}$ now shows that the anomalous ''fishtail'' behavior observed in the magnetic hysteresis essentially is related to the field component in the c-axis direction which is also a measure of the density of pancake vortices in the ab planes. The field component parallel to the CuO_2 planes, on the other hand, is much less relevant for pinning. Nevertheless, the exact origin of the ''fishtail'' is still unclear.

Figure 4(b) shows the scaled $\tau_{\rm irr}/B$ at $B=1.4$ T and for the temperatures $T=70.2$, 73.8, 75.0, and 76.8 K. With increasing temperature the position of the maximum shifts to lower fields B^c, and the peak width decreases. However, for $T=76.8$ K the shape of $\tau_{\rm irr}(\theta)$ is very different from the data taken at lower temperatures. The double peak, clearly seen for $T=70.2$, 73.8, and 75.0 K, has completely vanished, and $\tau_{\rm irr}$ is not longer decreasing as $B^c\to 0$. Instead of a minimum, $\tau_{\rm irr}$ exhibits now a maximum centered around $B^c=0°$ (or equivalently for $B\|ab$ plane), similar to that seen in the Al-doped sample. This demonstrates that the pinning nature is different below and above $T=76.8$ K which is our estimated 2D-3D crossover temperature $T_{\rm 2D\text{-}3D}$ for the clean 248 sample. Moreover, the anomalous maximum in the angle-dependent torque and the unusual magnetic hysteresis[13] appear to be closely related and to reflect the quasi-2D nature of the vortex core.

Another consequence of the layered structure of the cuprates is the possibility of an intrinsic pinning of vortex lines between the CuO_2 planes. The so-called lock-in of vortex lines is most pronounced in the reversible magnetization data. For this reason we discuss first the angle-dependent reversible torque within the framework of the 3D anisotropic model. We then show in Sec. V how the lock-in of vortex lines manifests itself as deviations from the 3D model.

IV. DETERMINATION OF SUPERCONDUCTING PARAMETERS

The determination of fundamental superconducting parameters such as the penetration depth λ, the upper critical field B_{c_2}, and the coherence length ξ is still a challenging experimental task. The standard extraction of these parameters from the isothermal magnetization $dM/d\ln H \propto 1/\lambda_{ab}^2(T)$ is restricted to the temperature regime close to T_c and therefore is affected by large vortex fluctuations. For the clean 248 crystal, however, the enhanced reversibility allows a measurement of the temperature dependence of the basic superconducting parameters λ_{ab}, $B_{c_2}^c$, γ, and ξ_{ab} even for temperatures much below T_c.

The theory of the angular dependence of the magnetic torque for anisotropic superconductors has been worked out in detail.[15,16] Based on the 3D anisotropic London model, the

reversible magnetic torque $\tau_{\rm rev}$ of an anisotropic superconductor of volume V is given by

$$\tau(\theta)_{\rm rev}=\frac{\Phi_0 VB}{16\pi\mu_0\lambda_{ab}^2}\,\frac{\gamma^2-1}{\gamma}\,\frac{\sin 2\theta}{\epsilon(\theta)}\ln\frac{\gamma\eta B_{c_2}}{B\epsilon(\theta)}, \qquad (2a)$$

$$\epsilon^2(\theta)=\cos^2\theta+\gamma^2\sin^2\theta, \qquad (2b)$$

where θ is the angle between the applied field B and the ab plane, Φ_0 is the flux quantum, $\gamma=\sqrt{m_c^*/m_{ab}^*}$ is the effective-mass anisotropy, B_{c_2} is the upper critical field in the c direction, and λ_{ab} is the effective in-plane penetration depth. The numerical parameter η is of the order of unity[17] and depends on the structure of the vortex line lattice. The angular dependence of $\tau_{\rm rev}$ therefore provides a direct and simultaneous measurement of $\lambda_{ab}(T)$, γ, and $\eta B_{c_2}(T)$, from which we can extract the coherence length $\xi_{ab}=\sqrt{\Phi_0/2\pi B_{c_2}}$ and the Ginzburg-Landau parameter $\kappa=\lambda_{ab}/\xi_{ab}$. In Eq. (2a) only the reversible magnetic torque arising from an equilibrium vortex line configuration is considered. In experiments, this condition is strictly fulfilled only for temperatures close to T_c or for fields $B>\gamma B_{\rm irr}$, where $B_{\rm irr}$ is the irreversibility field measured in the c direction. Nevertheless, if $\tau_{\rm irr}$ is clearly smaller than $\tau_{\rm rev}$, as is the case in our 248 sample, the decomposition according to Eq. (1) is appropriate.

We now analyze the reversible torque measured in the clean 248 sample within the framework of the 3D model given in Eq. (2). The fitting parameters are the anisotropy parameter γ, the critical field $\eta B_{c_2}(T)$, and the penetration depth $\lambda_{ab}(T)$. The latter depends strongly on the absolute value of the torque amplitude. Its accuracy is therefore governed by the correct determination of the superconducting volume of the sample and the calibration of the torque magnetometer, which is not the case for the two other parameters. In Fig. 5 the angle-dependent torque is shown for $T=76.8$ K and an applied field of $B=1.4$ T. The torque was monitored for both directions of rotation as indicated by the arrows, and was found to be almost perfectly reversible. Only for the field close to the ab plane ($\theta<6°$) was a small hysteresis observed [see Fig. 5(b)]. The reversible torque $\tau_{\rm rev}$ (crosses) derived by means of Eq. (1a) was very well fitted with Eq. (2a). The best fit was obtained by using the parameters $\gamma=12.3\pm0.1$, $\eta B_{c_2}(76.8\ {\rm K})=3.5\pm0.1$ T, and $\lambda_{ab}(76.8\ {\rm K})=448\pm25$ nm. The theoretical curve (solid line) describes the experimental data almost perfectly over the entire angular range. The quality of the fit is true even for $\theta<6°$, where the torque signal is slightly irreversible. The fit parameters are almost insensitive to the strength of the applied field. Even at $B=0.5$ T they are within the errors given above. The same analysis has been performed on the torque data taken at other temperatures. The results are shown in Fig. 6. The upper critical field ηB_{c_2} [Fig. 6(a)] increases linearly with decreasing temperature and has a slope of $\eta dB_{c_2}/dT=-1.86\pm0.06$ T/K. By using $\eta\simeq1$ its value at zero temperature is found through the relation $B_{c_2}(0)\simeq-0.69T_c(dB_{c_2}/dT)_{T_c}$ (Ref. 18) to be $B_{c_2}(0)\simeq90\pm10$ T. This gives an estimate of the in-plane coherence length of $\xi_{ab}(0)=\sqrt{\Phi_0/2\pi B_{c_2}(0)}\simeq1.9\pm0.1$ nm, which is

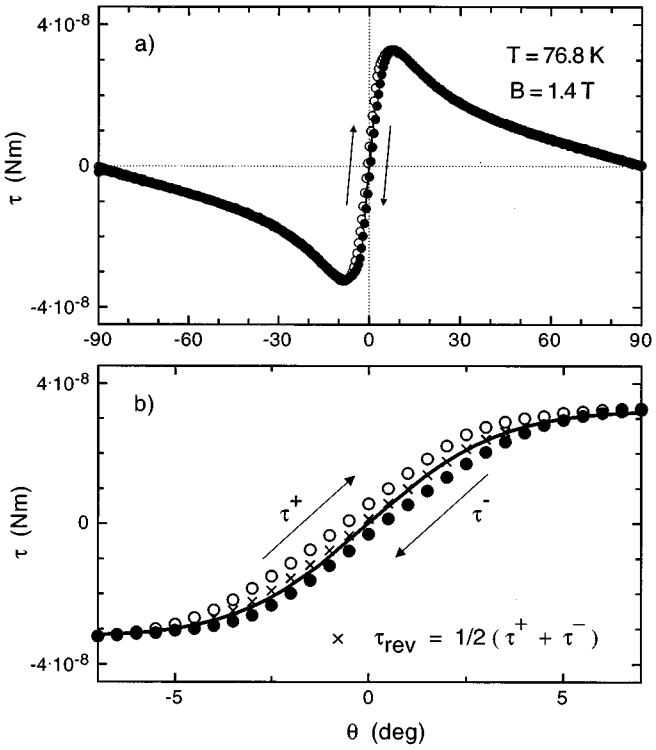

FIG. 5. (a) Angle-dependent torque for a ''clean'' 248 single crystal at $T=76.8$ K and $B=1.4$ T. The torque signal was monitored for both directions of rotation as indicated by the arrows. The solid line is the fit of the reversible torque data $\tau_{\rm rev}$ using Eq. (2a). The slight hysteretic behavior close to the ab plane is clearly seen on the enlarged scale in (b).

in good agreement with values reported from magnetization measurements on polycrystalline samples.[19,20] The effective-mass anisotropy parameter γ shown in Fig. 6(b) is found to be almost temperature independent ($11.0<\gamma<12.5$) and is close to the value of $\gamma\simeq10$ measured indirectly by Martinez *et al.*[21] The temperature dependence of $1/\lambda_{ab}^2$ is shown in Fig. 6(c). The solid line is a power law of the form $1/\lambda_{ab}^2(t)=1/\lambda_{ab}^2(0)(1-t^n)$. For a variable exponent n this empirical power law provides a good approximation for various theoretical models of $\lambda_{ab}(t)$. For instance, the weak-coupling BCS temperature dependence may be approximated with an exponent of $n\approx2.3$, whereas the two-fluid model corresponds to an exponent of $n=4$. The best fit to the data was obtained for $\lambda_{ab}(0)=143\pm15$ nm and for an exponent $n=3.6$, which is close to expectations for the two-fluid model and for an s-wave superconductor in the strong-coupling limit.[22] The fit produces a larger $T_c=79.8$ K than the actual measured value of $T_c=78.8$ K. However, by fixing $T_c=78.8$ K and using the simple two-fluid approach $n=4$ (dashed line) the extrapolated value of the penetration depth does not change. This λ_{ab} value is slightly smaller than those reported earlier between 160 nm and 200 nm.[19–21] However, by using the independently measured $\kappa=70.2$ from Ref. 23 and the above value of $\xi_{ab}=1.9$ nm, we obtain $\lambda_{ab}=\kappa\xi_{ab}=133$ nm, which is in reasonable agreement with our λ_{ab} obtained by torque magnetometry. Moreover, a recent far-infrared study on a 248 single crystal[24] revealed a large a/b anisotropy of the penetration depth ($\lambda_a=200$ nm,

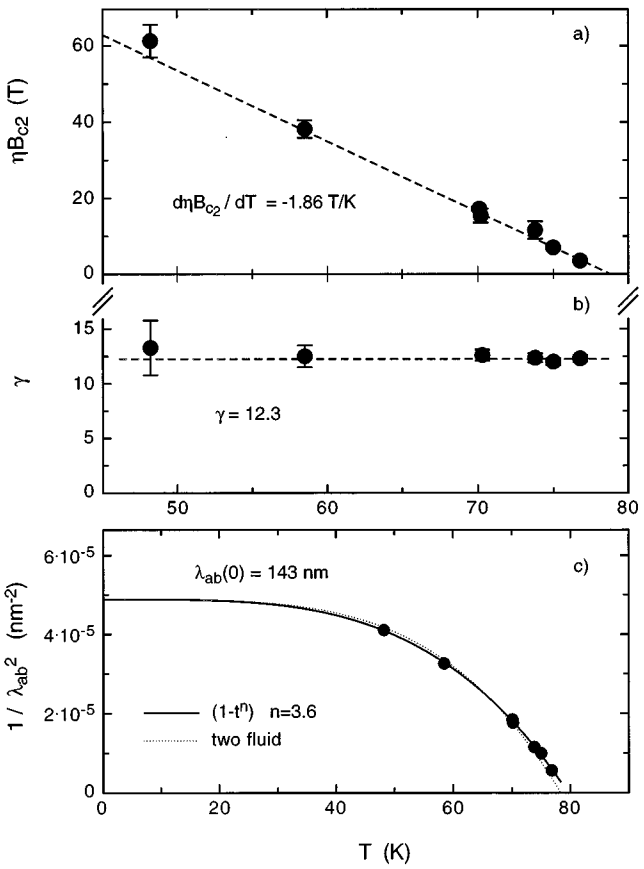

FIG. 6. Temperature dependence of the upper critical field ηB_{c_2} parallel to the c axis, of the effective mass anisotropy ratio γ, and of the penetration depth $1/\lambda_{ab}^2$ as derived from the reversible torque. The solid line in (c) corresponds to a power law of $1/\lambda_{ab}^2 \propto [1-(T/T_c)^n]$, where $n=3.6$. The dashed line corresponds to the two-fluid model ($n=4$).

$\lambda_b = 80$ nm). By simply taking the mean value in the two planar directions we obtain an effective $\lambda_{ab} = \sqrt{\lambda_a \lambda_b} \simeq 135$ nm, which is again close to our own result of $\lambda_{ab} = 143$ nm. A comparison of the characteristic superconducting parameters obtained by torque magnetometry with values reported in the literature is summarized in Table I.

In Eq. (2) thermal fluctuations of vortices are not considered. In fact they become important only for T close to T_c and/or for magnetic fields larger than the 3D-2D crossover field given by $B_{\rm cr} = \phi_0/(d\gamma)^2$, where d is the distance between neighboring CuO_2 blocks. Taking $d = 1.35$ nm and $\gamma = 12.3$, the crossover field for the 248 compound is $B_{\rm cr} \simeq 7.5$ T, a value much higher than that reached in our experiment. Moreover, the excellent fit of Eq. (2) to our data indicates that vortex fluctuations are not relevant here, in agreement with Ref. 20.

V. INTRINSIC PINNING AND THE LOCK-IN TRANSITION

A consequence of the layered structure of the cuprates is the intrinsic pinning of the vortex lines between the superconducting planes which we now discuss. The effect of the intrinsic pinning will be most pronounced in the reversible torque and will manifest itself as a deviation from the calculated reversible torque as obtained within the 3D anisotropic London model, Eq. (2). At very small angles $\theta < \theta_l$ it is energetically favorable for vortex lines to remain between the CuO_2 layers than to align with the applied field. The possibility of such confinement of vortices has been studied theoretically in detail.[4,25,26] One of the most direct consequence of this lock-in of vortex lines is the perfect screening of the c-axis component of the applied field, similar to the Meissner state, whereas for the ab-plane direction the field can almost fully penetrate. For $\theta < \theta_l$, the reversible torque may then be simply approximated by

$$\tau_{\rm rev}(\theta) = M_c B \cos\theta = \frac{HB}{1-N_c} \sin\theta\cos\theta, \qquad (3)$$

where N_c is the demagnetization factor in the c-axis direction. Here, the torque $M_{ab} B \sin\theta \simeq 0$ was not considered, because $M_{ab} \ll M_c$, which is true for $B \gg B_{c_1}$. For $\theta > \theta_l$ the expression given in Eq. (2) remains valid. The angular dependence of $\tau_{\rm rev}$ thus shows two maxima, one which is related to the anisotropy parameter γ and another much closer to the ab plane, which marks the onset of the lock-in of vortex lines between the CuO_2 planes. The relative size of these two maxima strongly depends on temperature.

The presence of a sharp second maximum close to the ab plane in the reversible torque is the most pronounced manifestation of the intrinsic pinning, but the experimental verification remains difficult.[8,27] Usually the presence of isotropic pinning either prevents the accommodation of vortex lines between the layers and/or the large irreversible magnetization completely masks the reversible magnetization. This is, however, not the case for our clean 248 material. Coming back to Fig. 2(c), the angle-dependent torque clearly shows

TABLE I. Comparison of characteristic superconducting parameters of $Y_2Ba_4Cu_8O_{16}$.

λ_{ab} (nm)	ξ_{ab} (nm)	κ	γ	Sample	Method	Ref.
143±15	1.9±0.1	76±12	12.3±0.5	crystal	torque	this work
180±20	4.0±1.0	45±10	10	Al-doped crystal	resistivity	21
166–188	2.38	70		oriented powder	magnetization	23
196	1.95	100		oriented powder	magnetization	19
197±30	1.93	112		powder	magnetization	20
160±15				powder	μSR	28
200(λ_a)				crystal	IR spectrosc.	24
80(λ_b)				crystal	IR spectrosc.	24

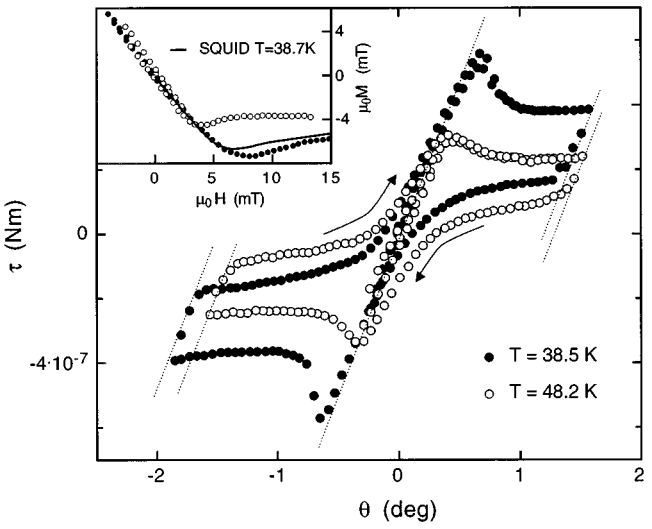

FIG. 7. Angle-dependent torque for the field close to the ab plane for an applied field of $B=0.5$ T and for $T=38.5$ K (solid symbols) and $T=48.2$ K (open symbols). Note that the slope $d\tau/d\theta$ for $\theta\simeq 0°$ is temperature independent. In the inset the magnetization data M_c obtained from the torque measurements are compared with SQUID magnetization measurements for the field B parallel to the c axis and for $T=38.7$ K (solid line).

two maxima: a first one at $\theta=8°$ related to the torque maximum in Eq. (2) and a second one in the form of a sharp peak very close to the ab plane. This second peak cannot be explained with the 3D model, but it could be associated with the onset of intrinsic pinning generated by the layered structure. To illustrate this further, a close-up view of $\tau(\theta)$ measured at $T=48.2$ and 38.5 K and in an applied field of $B=0.5$ T is shown in Fig. 7. Initially the field was applied in the ab plane, and progressive hysteresis measurements were performed by rotating the field in both directions. As long as $\theta<0.3°$ (0.7° for 38.5 K) the torque was completely reversible and linear in θ which is consistent with Eq. (3). When θ exceeds the peak angle of $\theta_l\simeq 0.3°$ (0.7° for 38.5 K) a small hysteretic behavior sets in as the vortex lines start to cross the CuO_2 planes. With decreasing temperature the second peak becomes more pronounced. However, the initial slope is *independent* of temperature, as it is expected for the $\tau(\theta)$ in the locked state [Eq. (3)]. In the inset of Fig. 7 low-field SQUID magnetization measurements with H parallel to the c axis are compared with the magnetization $M_c=\tau_{\rm rev}/B\cos\theta$ given in Eq. (3) and obtained from the angle-dependent torque measured at $T=48.2$ and 38.25 K. The two techniques determine an *identical* slope of $dM/dH=-16.2$ which corresponds to a demagnetization factor of $N_c=0.94$ which is reasonable given the platelike geometry of the sample. This suggests that a complete shielding of the field component in the c-axis direction takes place for both experiments. Because the applied field was $B=0.5$ T for the torque measurements, a complete shielding of the c-axis component of the applied field can only be achieved for a configuration where the vortex lines are indeed confined between the CuO_2 layers. The experimental finding of a temperature-independent magnetic torque for the field close to the ab plane and its linear dependence on the orientation θ are strongly suggestive for a lock-in of vortex lines between the CuO_2 planes.

VI. SUMMARY

In this work we have presented a detailed study of the angle-dependent torque in single-crystalline $Y_2Ba_4Cu_8O_{16}$. As a pristine material the 248 compound exhibits a remarkably low intrinsic disorder, which is clearly shown by the almost reversible torque, even for temperatures far below T_c. This allowed us to study the interplay between vortices and the inherent layered structure of the 248 material. We found that the 3D London model is appropriate as much as London screening currents are considered. However, this model cannot explain the unusual form of the irreversible torque. We found that the small and unusual form of the irreversible torque is basically determined by the c-axis component of the applied field. This suggests that while the vortex lines are continuous and straight, the vortex cores are fragmented into pancake vortices, which is true even for temperatures very close to T_c. We have further identified the 2D-3D crossover temperature $T_{\rm 2D\text{-}3D}=76.8$ K above which the 3D model adequately describes the reversible and irreversible torque. For temperatures $T<50$ K we report a sharp peak very close to the ab plane in the angle-dependent torque, which is identified as the lock-in of vortex lines between the CuO_2 layers. From the angular dependence of the reversible torque, which is very well described by the 3D anisotropic model, we obtain the effective mass anisotropy $\gamma\simeq 12.3$, the in-plane penetration depth of $\lambda_{ab}\simeq 143\pm 15$ nm, and an estimate of the coherence length $\xi_{ab}\simeq 1.9\pm 0.1$ nm of the 248 compound.

ACKNOWLEDGMENTS

We are very grateful to J. R. Clem and V. G. Kogan for helpful discussions concerning the anomalous angle-dependent torque data. This work was supported in part by Swiss National Science Foundation Grant No. NFP30.

*Present address: Ginzton Laboratory, Stanford University, Stanford, CA 94305.

[1] G. Blatter, M. V. Feigel'man, V. B. Geshkenbein, A. I. Larkin, and V. M. Vinokur, Rev. Mod. Phys. **66**, 1125 (1994).

[2] D. E. Farrell, J. P. Rice, D. M. Ginsberg, and J. Z. Liu, Phys. Rev. Lett. **64**, 1573 (1990).

[3] M. Tachiki and S. Takahashi, Solid State Commun. **72**, 1083 (1989).

[4] D. Feinberg and C. Villard, Mod. Phys. Lett. B **4**, 9 (1990).

[5] D. Feinberg, Physica C **194**, 126 (1992).

[6] T. Klupsch, R. Hergt, and R. Hiergeist, Physica C **211**, 65 (1993).

[7] B. Janossy, R. Hergt, and L. Fruchter, Physica C **170**, 22 (1990).

[8] V. Vulcanescu, G. Collin, H. Kojima, I. Tanaka, and L. Fruchter, Phys. Rev. B **50**, 4139 (1994).

[9] J. Karpinski, E. Kaldis, E. Jilek, S. Rusiecki, and B. Bucher, Nature **336**, 660 (1988).

[10] H. Schwer, J. Karpinski, E. Kaldis, G. I. Meijer, C. Rossel, and M. Mali, Physica C **267**, 113 (1996).

[11] D. Zech, Ph.D. thesis, University of Zurich, 1995.
[12] L. Fruchter and I. A. Campbell, Phys. Rev. B **40**, 5158 (1989).
[13] M. Xu, D. K. Finnemoe, G. W. Crabtree, V. M. Vinokur, B. Dabrowski, D. G. Hinks, and K. Zhang, Phys. Rev. B **48**, 10 630 (1993).
[14] G. Blatter, V. B. Geshkenbein, and A. I. Larkin, Phys. Rev. Lett. **68**, 875 (1992).
[15] L. J. Campbell, M. M. Doria, and V. G. Kogan, Phys. Rev. B **38**, 2439 (1988).
[16] V. G. Kogan, M. M. Fang, and S. Mitra, Phys. Rev. B **38**, 7049 (1988).
[17] Z. Hao and J. Clem, Phys. Rev. B **43**, 7622 (1990).
[18] N. R. Werthamer, E. Helfand, and P. C. Hohenberg, Phys. Rev. **147**, 295 (1966).
[19] W. C. Lee and D. M. Ginsberg, Phys. Rev. B **45**, 7402 (1992).
[20] G. Triscone, A. F. Khoder, C. Opagiste, J. Y. Genoud, T. Graf, E. Janod, T. Tsukamoto, M. Couach, A. Junod, and J. Muller, Physica C **224**, 263 (1994).
[21] J. C. Martinez, O. Laborde, J. J. Préjean, C. Chappert, J. P. Renard, J. Karpinski, and E. Kaldis, Europhys. Lett. **14**, 693 (1991).
[22] J. Rammer, Europhys. Lett. **5**, 77 (1988).
[23] J. Sok, M. Xu, W. Chen, B. J. Suh, J. Gohng, D. K. Finnemore, M. J. Kramer, L. A. Schwartzkopf, and B. Dabrowski, Phys. Rev. B **51**, 6035 (1995).
[24] D. N. Basov, R. Liang, D. A. Bonn, W. N. Hardy, B. Dabrowski, M. Quijada, D. B. Tanner, J. P. Rice, D. M. Ginsberg, and T. Timusk, Phys. Rev. Lett. **74**, 598 (1995).
[25] B. I. Ivlev, Y. N. Ovchinikov, and V. L. Pokrovskii, Mod. Phys. Lett. **5**, 73 (1991).
[26] A. E. Koshelev, Phys. Rev. B **48**, 1180 (1993).
[27] B. Janossy, A. de Graaf, P. H. Kes, and V. N. Kopylov, Physica C **235-240**, 2871 (1994).
[28] H. Keller, W. Kündig, I. M. Savic, H. Simmler, B. Stäuble-Pümpin, M. Warden, D. Zech, P. Zimmermann, E. Kaldis, J. Karpinski, S. Rusiecki, J. H. Brewer, T. M. Riseman, J. W. Schneider, Y. Maeno, and C. Rossel, Physica C **185-189**, 1089 (1991).